Coastal Education & Research Foundation, Inc.

Numerical Study of Meteo-tsunami Caused by High Pressure System in Winter Season
Author(s): Hyunsu Kim, Yoo-Keun Kim, Seung-Buhm Woo and Myung-Seok Kim
Source: *Journal of Coastal Research*, Special Issue No. 85: Proceedings of the 15th International Coastal Symposium, Haeundae, Busan, 13-18 May 2018 (2018), pp. 861-865
Published by: Coastal Education & Research Foundation, Inc.
Stable URL: https://www.jstor.org/stable/26488340
Accessed: 11-03-2024 08:28 +00:00

REFERENCES
Linked references are available on JSTOR for this article:
https://www.jstor.org/stable/26488340?seq=1&cid=pdf-reference#references_tab_contents
You may need to log in to JSTOR to access the linked references.

JSTOR is a not-for-profit service that helps scholars, researchers, and students discover, use, and build upon a wide range of content in a trusted digital archive. We use information technology and tools to increase productivity and facilitate new forms of scholarship. For more information about JSTOR, please contact support@jstor.org.

Your use of the JSTOR archive indicates your acceptance of the Terms & Conditions of Use, available at https://about.jstor.org/terms



Coastal Education & Research Foundation, Inc. is collaborating with JSTOR to digitize, preserve and extend access to *Journal of Coastal Research*

This content downloaded from 165.246.140.197 on Mon, 11 Mar 2024 08:28:57 +00:00
All use subject to https://about.jstor.org/terms

Journal of Coastal Research	SI	85	861–865	Coconut Creek, Florida	2018

Numerical Study of Meteo-tsunami Caused by High Pressure System in Winter Season

Hyunsu Kim[†], Yoo-Keun Kim[‡*], Seung-Buhm Woo[§], and Myung-Seok Kim[§]

[†]Division of Environment and Sustainability, Hong Kong University of Science and Technology, Kowloon, Hong Kong

[‡]Department of Atmospheric Sciences, Pusan National University, Busan, Republic of Korea

[§]Department of Ocean Sciences, Inha University, Incheon, Republic of Korea

www.cerf-jcr.org

www.JCRonline.org

ABSTRACT

Kim, H.; Kim, Y.-K.; Woo, S.-B., and Kim, M.-S., 2018. Numerical study on the meteo-tsunami caused by high pressure system in winter season. *In:* Shim, J.-S.; Chun, I., and Lim, H.S. (eds.), *Proceedings from the International Coastal Symposium (ICS) 2018* (Busan, Republic of Korea). *Journal of Coastal Research*, Special Issue No. 85, pp. 861–865. Coconut Creek (Florida), ISSN 0749-0208.

The Yellow Sea is the area of the world where meteo-tsunamis are frequent along with the Mediterranean. Kim *et al.* (2016) reported that most meteo-tsunami events occur in spring (~ 60%), but approximately 30% also occur in winter along the west coast of the Korean peninsula. Unlike meteo-tsunamis occurring in spring, a meteo-tsunami occurring in winter could be caused by mechanical atmospheric instability following the expansion of a high-pressure system like the Siberian high. In this study, Synoptic weather analysis was performed on some meteo-tsunami events during winter season. As a result, most of the meteo-tsunami events were caused by a discontinuity of the instability when the high-pressure system expanded to the west coast of the Korean peninsula.

ADDITIONAL INDEX WORDS: *Meteo-tsunami, Atmospheric instability, Siberian high, WRF, Numerical simulation.*

INTRODUCTION

The Yellow Sea is one of the areas of the world where meteo-tsunamis are frequent (Choi, Hwang, and Lee, 2014; Cho *et al*., 2013; Kim, Woo, and Eom, 2013). Many preliminary studies have shown that meteo-tsunamis occurring in coastal areas around the Korean peninsula are concentrated mainly in spring and the atmospheric instability by a low-pressure system or a mesoscale convective system is one of many reasons for meteo-tsunamis (Kim *et al*., 2017; Renault *et al.*, 2011; Šepić, Vilibić, and Belušić, 2009; Monserrat, Vilibić, and Rabinovich, 2006). Kim *et al.* (2016) reported that most meteo-tsunami events occurred in spring (~ 60%), but approximately 30% also occurred in winter along the west coast of the Korean peninsula. They emphasized that unlike the meteo-tsunamis occurring in spring, the meteo-tsunamis occurring in winter could be caused by mechanical atmospheric instability following the expansion of a high-pressure system, such as Siberian high. On the other hand, there have been relatively few studies on meteo-tsunamis caused by high-pressure systems up to now. In particular, Kim *et al.* (2016) reported that a detailed and definitive analysis, such as high-resolution weather modeling is somewhat insufficient. The synoptic weather analysis has an advantage in that it can easily know the overall pressure distribution at the time of the occurrence of a meteo-tsunami. Because the temporal and spatial resolution of the data used in synoptic weather analysis is low, it is limited to an analysis of the meteorological causes of meteo-tsunamis. In this study, to improve the understanding of meteo-tsunamis caused by the Siberian high in winter, the atmospheric structure during the events was analyzed in detail by performing numerical meteorological simulations. In addition, the results of this simulation were compared with synoptic analysis to clarify the causes of the meteo-tsunamis caused by high pressure systems in winter.

DOI: 10.2112/SI85-173.1 received 30 November 2017; accepted in revision 10 February 2018.

*Corresponding author: kimyk@pusan.ac.kr

©Coastal Education and Research Foundation, Inc. 2018

METHODS

Numerical simulations were carried out using the Advanced Research WRF (Weather Research and Forecast) model, which is used widely to predict the atmospheric conditions on the mesoscale or regional scale. The WRF model is based on fully compressible non-hydrostatic equations with a hydrostatic option and is expressed as a differential grid using the Arakawa-C horizontal grid staggering (Skamarock, *et al.*, 2008).

The 48 vertical layers were set closer to the ground to consider the instability of the lower and middle layers in synoptic analysis. The WRF modeling area was set considering the synoptic atmospheric flow, and the grid size for each domain was 30km, 10km, and 3.33km (Fig. 1). Table 1 lists the physical options used in the integration process. The background fields used as the input data of the WRF model were the FNL (final) data, which is the reanalysis data of the GFS (Global forecasting system) provided by the National centers for environmental prediction (NCEP). The FNL data has a spatial resolution of 1 ° × 1 ° and a time resolution of 6 hours. In addition, the sea surface temperature data of the FNL was replaced with the RTG-SST (Real time global SST) data to reduce the error of the initial conditions. The RTG-SST data has a spatial resolution of 0.5 ° × 0.5 ° and a time resolution of 24 hours. The modeling period was set to 6-days, including the day of the occurrence of the meteo-tsunami, and data for 5-days were used for the analysis except for the initial spin-up time (1-day).

This content downloaded from 165.246.140.197 on Mon, 11 Mar 2024 08:28:57 +00:00
All use subject to https://about.jstor.org/terms

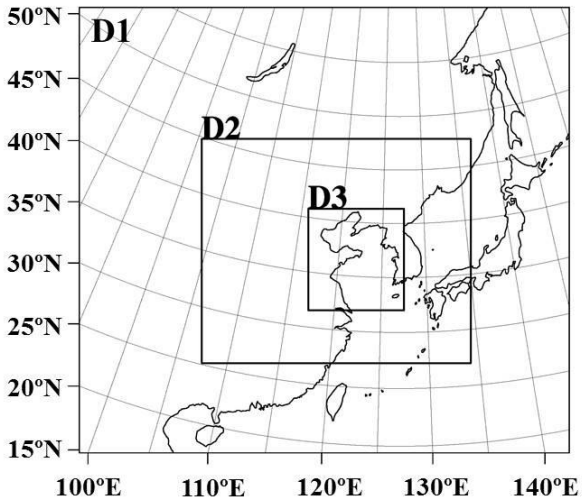


Figure 1. Map showing some of the horizontal grid nests (domain 1-3) used for the WRF.

Table 1. *Physical parameterizations of WRF model.*

	D1	D2	D3
Microphysics	WSM3 scheme	MYDM7 scheme	
Longwave radiation	RRTMG scheme		
Shortwave radiation	RRTMG scheme		
Surface layer	Revised MM5 surface layer scheme		
Land surface	Noah Land Surface Model		
Planetary boundary layer	YSU scheme		
Cumulus parameterization	Kain-Fritsch scheme		

RESULTS

To verify the performance of the WRF, the predicted values were compared with the representative ASOS observations (SW: Suwon, SS: Seosan, BY: Buyeo, GS: Gunsan, and MP: Mokpo). In time-series analysis, the trends of the observed variables (pressure, temperature, and wind speed) on the surface coincided with the values predicted for the representative meteo-tsunami event (00UCT, 18 Dec 2005 - 00UTC, 23 DEC 2005) in Winter (data not shown). The statistics, such as the IOA (index of agreement), MBE (mean bias error), RMSE (root mean square error), and Cor (correlation), were also presented to evaluate quantitatively the prediction accuracy of the numerical model (Table 2). The high IOA (0.89-0.95) and Cor(0.98-0.99) were calculated according to the surface pressure, which is one of the most important variables for a meteo-tsunami. Meanwhile, the MBE (-1.4-03.9 hPa) and RMSE (2.9-4.9 hPa) were relatively large because of the low prediction accuracy of the daily minimum values. Nevertheless, the WRF model was considered to be appropriate in this study because the predictive values generally reflected the observed trend.

Table 2. *Statistics of the weather variables to quantitatively evaluate the prediction accuracy of the WRF.*

ASOS	Pressure				Temperature				Wind speed			
	IOA	Cor	MBE	RMSE	IOA	Cor	MBE	RMSE	IOA	Cor	MBE	RMSE
SW	0.93	0.99	-2.3	4.0	0.79	0.84	2.4	3.2	0.80	0.77	1.1	1.7
SS	0.94	0.98	-1.4	3.4	0.59	0.76	4.3	5.0	0.78	0.71	1.3	2.2
GS	0.94	0.99	-1.8	3.5	0.64	0.65	2.8	3.5	0.70	0.61	1.0	1.8
MP	0.95	0.99	1.1	2.9	0.57	0.60	3.0	3.7	0.78	0.72	2.2	3.6
BY	0.89	0.99	-3.9	4.9	0.65	0.83	4.3	4.9	0.61	0.59	1.2	1.6
Ave.	0.93	0.99	-1.7	3.7	0.65	0.74	3.4	4.1	0.73	0.68	1.3	2.2

The sea level pressure and divergence of the wind at 10 m were used to analyze the atmospheric instability, which is the most important cause of a meteo-tsunami (Fig. 2). Generally, when a cold Siberian high expands extensively to the relatively warm Yellow Sea in winter, vertical atmospheric instability occurs due to the thermal difference between the atmosphere and ocean, and dynamic atmospheric instability occurs due to the strong stream line. At this time, low level cloud begins to develop from Bohai bay and expands to the west coast of the Korean peninsula in the form of a narrow street. Such strong atmospheric instability in a dense atmosphere can strengthen the sea level instability potentially. The discontinuity of the divergence line was analyzed off the coast of Gyeonggi Bay before the occurrence of the meteo-tsunami. This was attributed to the temporary change in the intensity of the stream line caused by the high pressure, which may affect the horizontal and vertical flow of the atmosphere in the surface boundary layer.

This content downloaded from 165.246.140.197 on Mon, 11 Mar 2024 08:28:57 +00:00
All use subject to https://about.jstor.org/terms

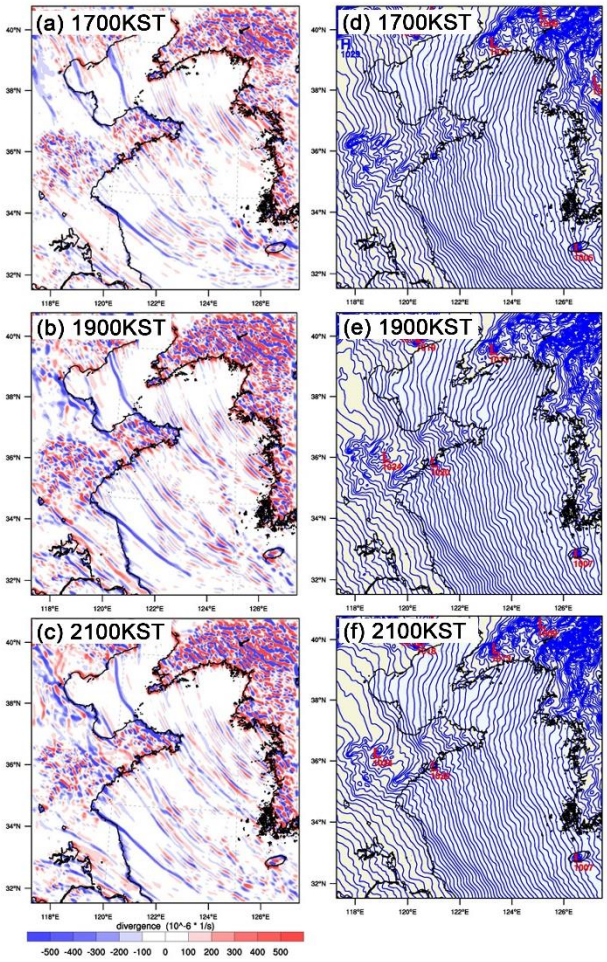


Figure 2. Spatial distribution of divergence at 10 m (left panel) and sea level pressure (right panel) computed by WRF model in 21 Dec ,2005.

The maximum radar reflectivity(MRR) was used to confirm the presence of the discontinuity (Fig. 3). The MRR, which is used mainly to identify precipitation, means the presence of rain clouds, and the inside of the rain clouds has a vertically unstable atmospheric structure. The MRR indicates more clearly the discontinuity in Gyeonggi Bay in Fig. 2. The discontinuity of the MRR is evidence that the intensity of the Siberian high has become stronger or weaker over time. To understand the vertical flow between upper and lower atmospheric layers, vertical cross-sections were analyzed for the discontinuity in unstable zone (Fig. 4). The red solid line in Fig. 4 was set for vertical cross-section analysis, and it passes through the area between the Shandong peninsula and Gyeonggi Bay where the discontinuity appears horizontally.

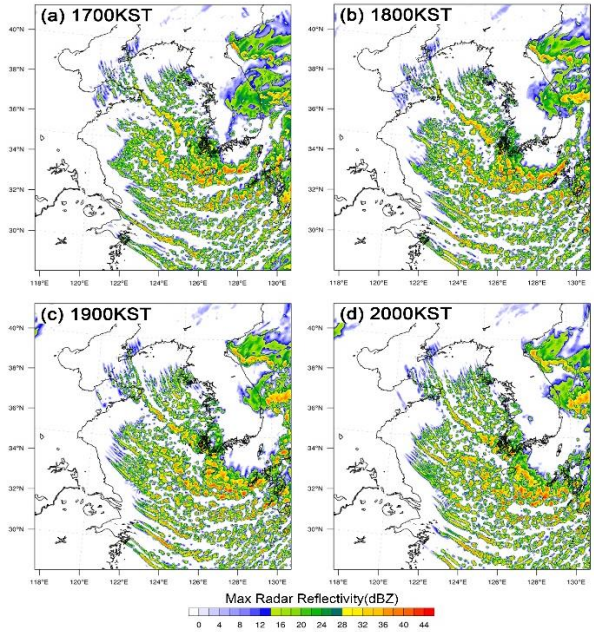


Figure 3. Spatial distribution of the maximum radar reflectivity computed by the WRF model in 21 Dec ,2005.

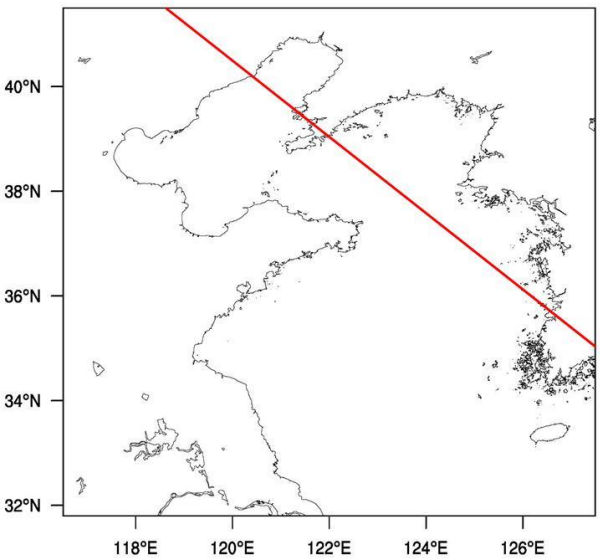


Figure 4. Map showing the cross-section line(red solid line) and coastal line used for vertical cross-section analysis of the WRF modeling results.

This content downloaded from 165.246.140.197 on Mon, 11 Mar 2024 08:28:57 +00:00
All use subject to https://about.jstor.org/terms

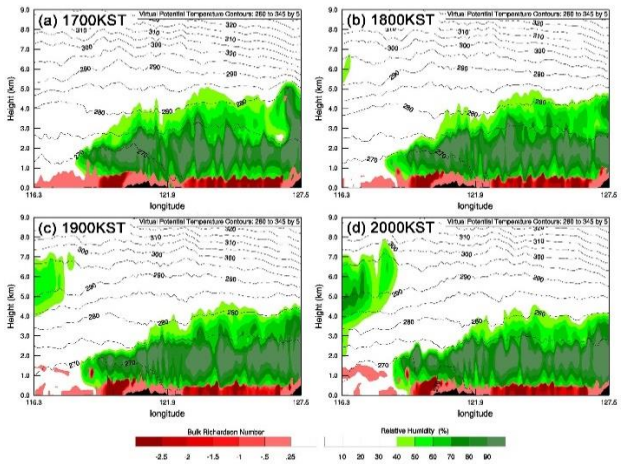


Figure 5. Cross-section distribution the relative humidity (%)(green contour), potential temperature (℃)(black solid line) and Richardson Number (<0.25)(red contour) along the cross-section line in Fig. 4, on 21 Dec 2005.

Fig. 5 shows the vertical cross-section to analyze the vertical atmospheric instability. The red zone represents a mechanically unstable zone where the Richardson number(Ri) is less than 0.25, the black solid line represents the virtual potential temperature, and the green zone represents the relative humidity.

A relative humidity range of more than 90% appears between about 1 and 3km, which is consistent with the above-mentioned low-level cloud being distributed in the form of a street from the Shandong Peninsula to the Korean peninsula. In addition, the distribution of the virtual potential temperature is represented by a substantial constant in the marine atmospheric boundary layer below 3 km. This means that the layer is well mixed vertically. In the Yellow Sea, particularly near the Korean peninsula, the Ri value is lower, indicating that the dynamic atmospheric instability is high in the coastal area.

On the other hand, in 1900 KST, the value of Ri increased temporarily and it decreased again in 2000 KST. This means the intensity of vertical atmospheric instability varies with time. At this time, the dynamic atmospheric instability layer with a Ri value lower than 0.25 appears as a wave form, which means that it is likely to affect the sea level fluctuations horizontally.

DISCUSSION

The numerical weather modeling for meteo-tsunami events during winter show that the discontinuity occurs when the Siberian high temporarily weakens and then strengthens in the Yellow Sea, *i.e.*, when expansion and contraction are repeated. Vertical cross-section analysis of this discontinuity shows that strong atmospheric instability occurs vertically in the atmospheric boundary layer, and the discontinuity due to the expansion of the high pressure appears to play a crucial role in causing the instability of the atmospheric boundary layer above sea level. This atmospheric instability causes sea level fluctuations in the open sea and propagates to the coast to cause resonance, which increases the probability of the occurrence of a meteo-tsunami.

CONCLUSIONS

Synoptic weather analysis was performed on some meteo-tsunami events during winter. As a result, most meteo-tsunami events in winter occurred when a high-pressure system expanded to the west coast of the Korean peninsula. The cold Siberian high expanded to the warm Yellow Sea, which causes low level cloud in the form of a narrow street with strong atmospheric instability above the marine atmospheric boundary layer. On the other hand, a discontinuity of the instability area is sometimes caused by the difference in instability of the Siberian high temporarily. This can affect the horizontal and vertical flow of the atmosphere in the marine boundary layer. This atmospheric instability caused by a high pressure system can increase the likelihood of occurrence of a meteo-tsunami in winter.

ACKNOWLEDGMENT

This work was funded by the Korea Meteorological Administration Research and Development Program under Grant KMIPA 2015-1073.

LITERATURE CITED

Cho, K.-H.; Choi, J.-Y.; Park, K.-S.; Hyun, S.-K.; Oh, Y., and Park, J.-Y., 2013. A synoptic study on tsunami-like along the west coast of Korea using an unstructured-grid ocean model. In: Conley, D.; Masselink, G.; Russell, P., and O'Hare, T. (eds.), *Proceedings, International Coastal Symposium 2013. Journal of Coastal Research*, Special Issue No. 65, pp. 678-683.

Choi, B.-J.; Hwang, C., and Lee H., 2014. Meteotsunami-tide interactions and high frequency sea level oscillations in the eastern Yellow Sea. *Journal of Geophysical Research: Oceans*, 119, 6725-6742, doi: 10.1002/2013JC009788.

Kim, H.; Kim, M.-S.; Kim, Y.-K.; Yoo, S.-H., and Lee, H.-J., 2017. Numerical weather prediction for mitigating the fatal loss by the meteo-tsunami incidence on the west coast of Korean Peninsula. In: Lee, J.L.; Griffiths, T.; Lotan, A.; Suh, K.-S., and Lee, J. (eds.), *Proceedings, The 2nd International Water Safety Symposium. Journal of Coastal Research*, Special Issue No. 79, pp. 119-123.

Kim, H.; Kim, M.-S.; Lee, H.-J.; Woo, S.-B., and Kim, Y.-K., 2016. Seasonal Characteristics and Mechanisms of Meteo-tsunamis on the West Coast of Korean Peninsula. In: Vila-Concejo, A.; Bruce, E.; Kennedy, D.M., and McCarroll, R.J. (eds.), *Proceedings of the 14th International Coastal Symposium* (Sydney, Australia). *Journal of Coastal Research*, Special Issue No. 75, pp. 1147 - 1151.

Kim, M.-S.; Woo, S.-B., and Eom, H.-M., 2013. Propagation of abnormal waves on 25 April 2008 at the West Coast of South Korea. In: Conley, D.; Masselink, G.; Russell, P., and O'Hare, T. (eds.), *Proceedings, International Coastal Symposium 2013. Journal of Coastal Research*, Special Issue No. 65, pp. 731-735.

Monserrat S.; Vilibić, I., and Rabinovich, A. B., 2006. Meteotsunamis: atmospherically induced destructive ocean waves in the tsunami frequency band. *Natural Hazards and Earth System Science*, 6(6), 1035-1051.

This content downloaded from 165.246.140.197 on Mon, 11 Mar 2024 08:28:57 +00:00
All use subject to https://about.jstor.org/terms

Renault, L.; Vizoso G.; Jansá A.; Wilkin J., and Tintoré J., 2011. Toward the predictability of meteotsunamis in the Balearic Sea using regional nested atmosphere and ocean models, *Geophys. Res. Lett.*, 38, L10601, doi:10.1029/2011GL047361.

Šepić, J.; Vilibić, I., and Belušić, D., 2009. Source of the 2007 Ist meteotsunami (Adriatic Sea), *J. Geophys. Res*., 114, C03016, doi:10.1029/2008JC005092.

This content downloaded from 165.246.140.197 on Mon, 11 Mar 2024 08:28:57 +00:00
All use subject to https://about.jstor.org/terms